Parity-fluctuation induced enlargement of the ratio Δ_E/k_BT_c in metallic grains

M. D. Croitoru,[1] A. A. Shanenko,[2] F. M. Peeters,[2] and V. M. Axt[3]

[1]*Laboratoire Onde et Matière d'Aquitaine, UMR 5798 du CNRS, Université Bordeaux 1, F-33405 Talence, France*

[2]*Departement Fysica, Universiteit Antwerpen, BE-2020 Antwerpen, Belgium*

[3]*Institut für Theoretische Physik III, Universität Bayreuth, DE-95440 Bayreuth, Germany*

(Received 20 May 2011; revised manuscript received 4 September 2011; published 15 December 2011)

We investigate how the interplay of quantum confinement and particle number-parity fluctuations affects superconducting correlations in ultra-small metallic grains. Using the number-parity projected BCS formalism we calculate the critical temperature and the excitation gap as a function of the grain size for grains with even and odd number of confined carriers. We show that the experimentally observed anomalous increase of the coupling ratio Δ_E/k_BT_c with decreasing superconducting grain size can be attributed to an enhancement of the number-parity fluctuations in ultra-small grains.

DOI: 10.1103/PhysRevB.84.214518 PACS number(s): 74.78.Na, 74.20.Fg

I. INTRODUCTION

Quantum confinement has a profound impact on the characteristics of nanostructured superconductors.[1–14] The main feature that distinguishes nanoscale superconductors from their homogeneous bulk counterparts is the discretization of the electronic energy bands. This effect has attracted a lot of interest especially in the past two decades due to the discovery of several novel phenomena in nanoscale samples, like an increase of the critical temperature in nanowires,[13] quantum-size oscillations of the superconducting temperature and of the perpendicular upper critical field in metallic nanofilms,[15–17] reaching the sample size limit where superconductivity breaks down, and the number parity effects in nanoparticles.[18,19] Another consequence of quantum confinement is a nonuniform spatial distribution of the superconducting order parameter $\Delta = \Delta(\mathbf{r})$ due to the breaking of the translational invariance along the confined dimensions. The importance of this issue was investigated in Refs. 20–23.

Confinement effects on superconducting correlations are especially pronounced in quasi-OD objects, as the electron confinement affects all spatial dimensions. The energy spectrum in such samples takes the form of a sequence of discrete levels with average energy spacing $\delta \approx 2\pi^2\hbar^2/m\,k_F\,V$, which is a fundamental energy scale in ultra-small grains. Since the end of the 1960s, when Giaever and Zeller in their pioneering work performed tunneling studies of large ensembles of superconducting particles,[24] most of the experiments devoted to superconducting correlations in grains were performed with grain powders,[25,26] or with granular films, where each metallic crystallized grain is surrounded by an insulating, amorphous coating (barrier), like Pb-PbO, Sn-SnO_x, Al-Al_2O_3, Al-Ge.[27–31] A remarkable feature of granular superconductors is the size dependent increase of the critical temperature. Within the single-electron tunneling spectroscopy technique Ralph *et al.*[18,19] measured a discrete electron spectrum for a single metallic grain and managed to identify a spectroscopic gap that was due to the presence of superconducting correlations, because this gap was larger than the average level spacing in an individual Al grain.

Recently, STM methods were used to detect the superconducting gap in a single physically isolated ultra-small grain.[32] These studies traced the size evolution of superconductivity in single, isolated lead nanoparticles that were grown on a BN/Rh substrate where the BN is an ultrathin layer which is insulating with a band gap of 6 eV and hence it efficiently decouples particles in the grain from those in the metallic Rh(111) substrate. These experiments revealed new effects as, for instance, a nonmonotonic variation of the coupling ratio $\zeta = \Delta_E/k_BT_c$, where T_c denotes the critical temperature and Δ_E is the energy gap, measured usually as a spectral gap, for example, via tunneling conductance experiments. It turns out that ζ first increases with a decrease of the particle size and then drops down when the particle size approaches the Anderson limit. Another experiment[31] reported on the size evolution of superconductivity in nanostructured granular Pb films consisting of crystalline Pb grains separated by an amorphous Pb-O phase, so the system behaves like a disordered network of weakly coupled grains. The authors observed that the coupling ratio ζ in these samples shows a simple increase with decreasing superconducting grain size and attributed this effect to the phonon softening at the surface.

These observations posed several interesting questions. Which is the mechanism behind the observed variation of the coupling ratio in small particles? Does the increase of ζ in both experiments have the same origin? Is it found only in strongly coupled superconductors?

In fact, a strong increase of the coupling ratio in the Pb-PbO granular film can be a manifestation of a superconducting insulator regime. As was shown in Ref. 33 in a strongly disordered granular superconductor an anomalously large single-particle excitation gap develops due to electronic correlations in the superconducting state near the superconductor-insulator transition and persists, even increases, in the insulating state long after superconductivity is destroyed. Since the gaps measured in tunneling experiments are usually identified with the superconducting gap an anomalously large ratio Δ_E/k_BT_c is predicted. However, it is not clear whether this mechanism can explain the increase of the coupling ratio observed in single isolated grains.

The present work provides an alternative explanation of the size-dependent increase of the coupling ratio which is suitable for a single isolated superconducting grain. Our paper is organized as follows. In Sec. II we briefly outline the formalism. Details are given in the Appendices. In Sec. III

we present our numerical results. A short summary and a discussion of the main findings are given in Sec. IV.

II. GENERAL SETTING AND FORMALISM

Dealing with a single isolated superconducting grain requires a few considerations concerning the adequate choice of description. On the one hand, in the experiment the electrons are confined within a grain. On the other hand, the electrostatic charging energy is negligible as the resistance between the grain and substrate is much smaller than the quantum of resistance.[34] In particular the fact that the particle is isolated puts some limitations on the possible formalism to use. The standard BCS theory is a grand canonical description and is valid for large enough samples with small relative fluctuations of the electron number. In ultra-small nanograins also quantum fluctuations of the pairing can become too large to be ignored. The use of a canonical ensemble description becomes more appropriate. Over the years a large number of methods has been developed,[35–39] which restore the violation of the particle number in the mean-field description. Since in practice it is hard to use these methods for rather large samples with more than 10^4 carriers and it is easier to define the order parameter as the amplitude to create/destroy a Cooper pair in the condensate we employ the parity-projected grand canonical description.[40–42] It appears that an improvement over BCS physics of pairing can be obtained by fixing the correct electrons' number parity while keeping the grand canonical description to force the average number of electrons to have the correct value. This formalism allows us to account for parity fluctuations. Another reason for the use of the parity-projected BCS formalism in our study is the fact that the deviation of the BCS parameter ζ from its standard BCS value of 1.76 is observed already at grain thicknesses $D \gtrsim 10$ nm, which is well above the Anderson limit, or the crossover between the conventional superconducting regime and the fluctuation-dominated regime of superconductivity.[7,43,44] At the same time the experiments from Refs. 45 and 46 revealed an even-odd asymmetry which takes place even in superconducting islands with macroscopically ($\gtrsim 10^8$) large number of electrons. Therefore the grain thicknesses for which an increase of the coupling ratio is observed fall into the domain where parity effects are observed.

For simplicity we consider a system with weak electron-electron interaction, for example, a Sn superconducting grain. Therefore we describe the grain by the following reduced BCS Hamiltonian, where only the time-reversal states are paired

$$\widehat{H} = \sum_{p,\sigma} \varepsilon_p a^\dagger_{p,\sigma} a_{p,\sigma} - \sum_{p,q} V_{p,q} a^\dagger_{p\uparrow} a^\dagger_{\overline{p}\downarrow} a_{\overline{q}\downarrow} a_{q\uparrow}. \tag{1}$$

Here p,q are integers numbering the single-particle energy levels ε_p and the operator $a_{p,\sigma}$ ($a^\dagger_{p,\sigma}$) annihilates (creates) an electron in state p with spin σ. The interaction matrix element V_{qp} is given by

$$V_{qp} = g \int \mathrm{d}^3 r \, |\varphi_q(\mathbf{r})|^2 \, |\varphi_p(\mathbf{r})|^2, \tag{2}$$

with g denoting the coupling constant and $\varphi_q(\mathbf{r})$ the single-electron wave function. The first term in Eq. (1) contains the single-electron energies, and the second term is the attractive (when $g > 0$) pairing interaction due to the exchange of virtual phonons. The interaction term scatters a pair of electrons from $(q\uparrow, \overline{q}\downarrow)$ to $(p\uparrow, \overline{p}\downarrow)$. Here we have assumed that the electron-electron interaction is unaffected by quantum confinement and it is the same as in bulk. In bulk the real interelectron potential is well approximated by a δ-function pseudopotential. Employing such a simplified interaction requires a regularization, which makes the matrix elements nonzero only between states within a narrow shell around the Fermi surface. Throughout this paper we assume zero magnetic field, so that the electron states can be chosen to be invariant under a time-reversal transformation.

Because of Kramers degeneracy (due to the time-reversal symmetry) of the single-electron states the properties of nanograins with odd and even number of electrons are different. To study the equilibrium properties of these distinct situations we employ a grand canonical partition function to constrain the average particle number, in which we enforce exactly the correct number parity η

$$Z_\eta = \mathrm{Tr}[\widehat{P}_\eta e^{-\beta(\widehat{H}-\mu\widehat{N})}], \tag{3}$$

where η is equal to $+1$ for even systems and -1 for odd ones. The projection operator which extracts the correct number parity component out of a state is

$$\widehat{P}_\eta = \tfrac{1}{2}(\widehat{1} + \eta e^{i\pi\widehat{N}}), \tag{4}$$

which suppresses states with the wrong number parity in the statistical ensemble.

By performing the Bogoliubov transformation[47]

$$\widehat{\gamma}_{\overline{p}} = u_p \widehat{a}_p - v_p \widehat{a}^+_{\overline{p}}, \tag{5}$$

$$\widehat{\gamma}_p = u_p \widehat{a}_{\overline{p}} + v_p \widehat{a}^+_p, \tag{6}$$

with the condition $|u_p|^2 + |v_p|^2 = 1$, the saddle-point approximation gives us the number-parity projected BCS equations

$$E_p = \widetilde{E}_p - \frac{2\eta R_\pi}{t_p - \eta R_\pi t_p^{-1}} \left[\mathcal{K} + \frac{\left(\Delta^\pi_p - \Delta^0_p\right)}{t_p + \eta R_\pi t_p^{-1}} \frac{\Delta^\eta_p}{\widetilde{E}_p} \right], \tag{7}$$

$$\Delta^\pi_p - \Delta^0_p \equiv \sum_q V_{pq} \frac{\Delta^\eta_q \left(t_q^{-1} - t_q\right)}{2\widetilde{E}_q}, \tag{8}$$

$$\Delta^\eta_p = \sum_q V_{pq} \frac{\Delta^\eta_q t_q}{2\widetilde{E}_q} \left[1 - \frac{\eta R_\pi t_p^{-2}\left(1 - t_q^{-2}\right)}{1 + \eta R_\pi t_p^{-2}} \right], \tag{9}$$

where $\widetilde{E}_p = \sqrt{\xi_p^2 + |\Delta^\eta_p|^2}$ [Eq. (A59)], and $\mathcal{K}$, ηR_π, and t_p are given by Eqs. (A66), (A27), and (A34), respectively. The sum in Eqs. (8) and (9) runs over the states with single-electron energy, measured from the chemical potential level, lying within the Debye window $\xi_p \in [-\hbar\omega_D, \hbar\omega_D]$, with ω_D the Debye frequency. For the sake of completeness we include the derivation of Eqs. (7)–(9) in the Appendices A. If η is replaced by zero, Eqs. (7) and (8) reduce to the usual BCS ones. Here it is worth noting that the quantities E_p and Δ^η_p are equal to their BCS values plus parity-projected corrections, and do not have a simple interpretation in terms of excitation energies and gaps as in the BCS case.

For a given number N_e of electrons in the grain the chemical potential μ is determined from equation

$$N_e = \sum_p f_p \left(1 - \frac{\xi_p}{E_p}\right) + (1 - f_p)\left(1 + \frac{\xi_p}{E_p}\right). \quad (10)$$

Here $f_p = (1 - t_p)/2$ is the Fermi distribution. For conventional superconductors the energy gap is typically much smaller than the chemical potential. As a result, μ stays nearly the same when passing from the normal state to the superconducting one.[48] Therefore, for large nanograins we evaluate Eq. (10) in the limit of vanishing superconducting order ($\Delta = 0$) before starting the main procedure of numerically solving Eqs. (7)–(9).

Equations (7)–(10) were solved numerically by iterations until full self-consistency was reached. At the first iteration the bulk value for the anomalous mean-field potential $\Delta_p = \Delta_{\text{bulk}}$ was taken. In the case of strong deviations of the chemical potential from its bulk value (which is the case for very small grains), the iterative procedure was repeated for various μ until the mean electron number was obtained.

Having solved self-consistently Eqs. (7)–(9), the spatial distribution of the order parameter can be obtained from (see Appendix B)

$$\Delta_\eta(\mathbf{r}) = g \sum_p \mathcal{U}_p(\mathbf{r})\, \mathcal{V}_p^*(\mathbf{r})\, \frac{t_p + \eta R_\pi t_p^{-1}}{1 + \eta R_\pi}. \quad (11)$$

Within the reduced BCS model considered here the particle-like $\mathcal{U}_p(\mathbf{r})$ and hole-like $\mathcal{U}_p(\mathbf{r})$ wave functions read

$$\mathcal{U}_p(\mathbf{r}) = u_p\, \varphi_p(\mathbf{r}), \quad \mathcal{V}_p(\mathbf{r}) = v_p\, \varphi_p(\mathbf{r}), \quad (12)$$

with $\varphi_p(\mathbf{r})$ denoting the single electron wave function and u_p and v_p defined either by Eqs. (5) and (6), or equivalently by

$$u_p^2 = \langle \mathcal{U}_p | \mathcal{U}_p \rangle = \int_V d\mathbf{r}\, \mathcal{U}_p^2(\mathbf{r}), \quad (13)$$

$$v_p^2 = \langle \mathcal{V}_p | \mathcal{V}_p \rangle = \int_V d\mathbf{r}\, \mathcal{V}_p^2(\mathbf{r}), \quad (14)$$

where V is the volume of the grain. Hence

$$\Delta_\eta(\mathbf{r}) = g \sum_p |\varphi_p(\mathbf{r})|^2 \frac{\Delta_p^\eta}{2\widetilde{E}_p} t_p \left(1 - \eta R_\pi \frac{1 - t_p^{-2}}{1 + \eta R_\pi}\right), \quad (15)$$

where the sum runs over all states with single-electron energies within the Debye shell.

In this paper we model the superconducting nanoparticle by a hard-wall box with sizes L_x, L_y, L_z. Due to quantum confinement the single electron wave function in such a grain reads

$$\varphi_p(x,y,z) = \prod_{l=x,y,z} \sqrt{\frac{2}{L_l}}\, \sin\left(\pi j_l \frac{r_l}{L_l}\right), \quad (16)$$

where $p = \{j_x, j_y, j_z\}$.

III. RESULTS AND DISCUSSION

Numerical calculations were performed with the set of parameters typical for tin:[49] $\hbar\omega_D/k_B = 195$ meV, $gN(0) = 0.25$, with $N(0)$ being the bulk density of states at the Fermi level and we used the bulk electron density[48] $n_e = 148\ \text{nm}^{-3}$. In the rest of the article we consider a nearly cubic grain with $L_x = D + a$, $L_y = D - a$, and $L_z = D$, where we will vary the thickness of the grain D and take $a = 0.2$ nm. Parallelepiped-shaped grains were taken in order to avoid strong degeneracy of the single-electron levels typical for the highly symmetric samples.

Figure 1 shows the critical temperature as a function of the superconducting grain thickness, calculated for an even (upper panel) and an odd (lower panel) number of electrons in the grain, respectively. The calculations were done for a thickness step of $\Delta D = 0.001$ nm. For each thickness the critical temperature was defined as the temperature above which the spatially averaged order parameter $\Delta_\eta = \langle \Delta_\eta(\mathbf{r}) \rangle$ becomes smaller than 0.01 of its value at $T = 0$. In both considered cases the numerical results exhibit two general features typical for the size-dependent pairing in high-quality

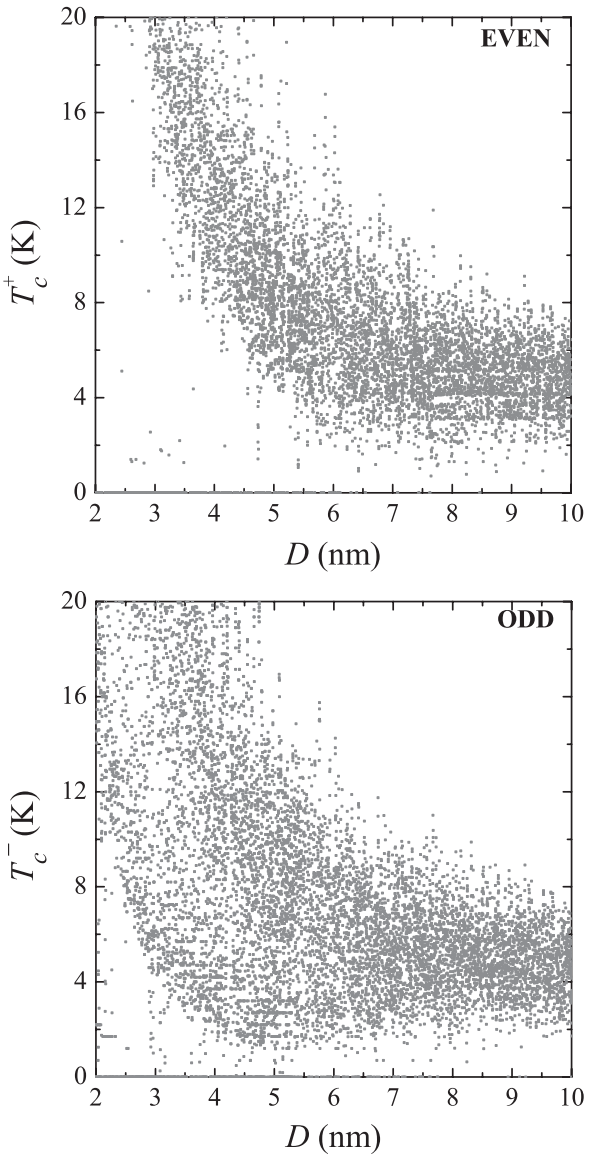

FIG. 1. Superconductor critical temperature as a function of the grain thickness: (upper panel) even-N_e grain; (lower panel) odd-N_e grain.

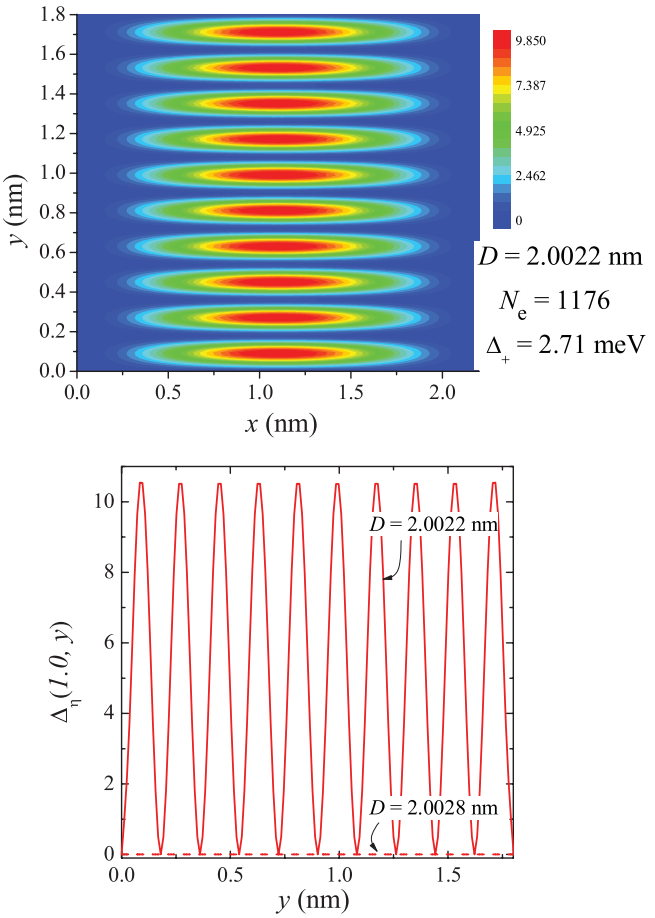

FIG. 2. (Color online) Lower panel: Spatial distribution of the pairing parameter $\Delta_\eta(\mathbf{r})$ in a grain containing an even number ($N_e = 1176$) of electrons. Upper panel: Spatial distribution of this parameter at $x = 1$ nm with an even ($N_e = 1176$, solid line) and odd number ($N_e = 1177$, dashed line) of electrons.

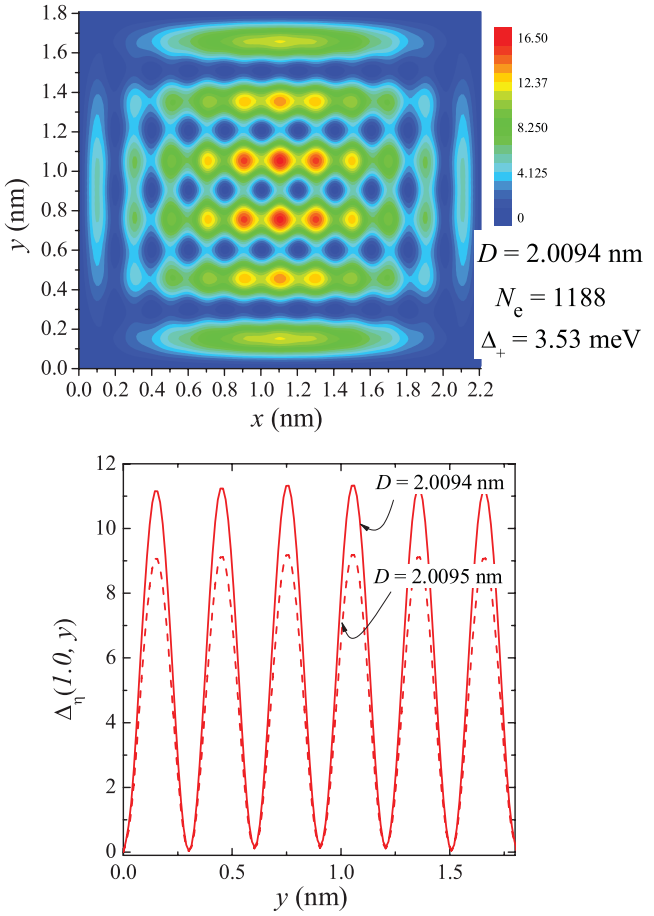

FIG. 3. (Color online) Upper panel: Spatial distribution of the pairing parameter $\Delta_\eta(\mathbf{r})$ in a grain containing an even number ($N_e = 1188$) of electrons. Lower panel: Spatial distribution of this parameter at $x = 1$ nm with an even ($N_e = 1188$, solid line) and odd number ($N_e = 1189$, dashed line) of electrons.

superconducting particles. First, we observe an overall increase of T_c with decreasing D. For large grain sizes the critical temperature approaches its bulk value, which for the here chosen parameters is $T_c^B = 4.01$ K. Second, the superconducting transition temperature fluctuates strongly.

Qualitatively, the fluctuating behavior of the superconducting temperature can be understood in the following way. The pair correlations are different from zero only within a finite range marked by the Debye window around the chemical potential μ. Moreover, the main contributions to the sum in Eq. (9) come from the states in the vicinity of the Fermi level, because here the expression $\Delta_p^\eta/\sqrt{\xi_p^2 + |\Delta_p^\eta|^2} \simeq 1$ ($\xi_p \simeq 0$). When varying the size of the grain, the number of states in the Debye window changes abruptly. The smaller the grain, the smaller the number of relevant states contributing to pair correlations. As a consequence, any superconducting quantity exhibits quantum-size oscillations.[12]

Let us now turn to the investigation of the differences observed in the critical temperature between grains with even and odd number of electrons. As seen in Fig. 1 for grains with widths larger than 6–8 nm the band over which T_c varies has lower and upper boundaries which are almost equal for both, even and odd parity. However, in the limit of ultra-small grains the lower boundary for the odd case is much smaller than that for the even case.

Before highlighting the physics behind these differences, let us give an additional example for a parity dependent feature which is most clearly seen for ultra-small grains. Figure 2 illustrates the typical space distribution of the pairing (order) parameter in superconducting nanograins. In this particular case the calculations were performed for grains with thicknesses $D = 2.0022$ nm and $D = 2.0028$ nm for $L_z = D/2$ at $T = 0.5$ K. The first grain contains an even number ($N_e = 1176$, upper panel) of electrons and the second one an odd number ($N_e = 1177$) of electrons. The lower panel displays the order parameter variations at $x = 1$ nm for these two grain sizes. The spatial distribution of the pairing is strongly inhomogeneous. It is clearly seen that there is a significant difference in the absolute value of the order parameter in these two grains. In the even case the spatially averaged order parameter has a value of $\Delta = 2.71$ meV, while in the odd case it is more than two orders of magnitude smaller. Notice that this difference resulted entirely from increasing the thickness of the system slightly such that only one extra electron was added to the grain. Figure 3 shows the spatial distribution of the pairing parameter in grains with thicknesses $D = 2.0094$ nm (upper

panel) and $D = 2.0095$ nm (lower panel) for $L_z = D/2$ at $T = 0.5$ K. In this case the order parameter in the grain with an odd number of electrons is comparable with the even case with only a difference of ≈20%.

The reason for the parity dependence in both examples can be understood as follows. At zero temperature, in the case of an even grain $\eta = +1$ Eq. (9) reduces to[40]

$$\Delta_q^+ = \sum_p V_{qp} \frac{\Delta_p^+}{2E_p}. \tag{17}$$

Denoting by f the index of the single-electron level whose energy ε_f is closest to the chemical potential μ, we obtain in the odd case $\eta = -1$ for $q \neq f$,

$$\Delta_{q\neq f}^- = \sum_{p\neq f} V_{qp} \frac{\Delta_p^-}{2E_p} \tag{18}$$

and (for $q = f$)

$$\Delta_{q=f}^- = \sum_{p\neq(f,f+1)} V_{f,p} \frac{\Delta_p^-}{2E_p}. \tag{19}$$

For the even case Eq. (17) exactly coincides with the standard BCS result. However, in the odd case, the level $p = f$ in the sum of Eq. (18) is absent, that is, it is not available for pairing. Pair correlations are present only within the Debye window around the chemical potential μ and are strongest for the level which is closest to μ.[50] In the odd case the ground state is obtained by creating one quasiparticle on this level above the BCS vacuum, and hence this unpaired electron forbids pair scattering involving this level. In nuclear physics the above approximation is usually referred to as the blocking (Soloviev) approximation.[51] The blocking of the $(f, \overline{f})$-pair formation may lead to a significant decrease of the pairing gaps. When the number of levels in the Debye window is small and the distance between these levels is of the order of the pairing gaps, inhibition of superconducting pairing may occur. This situation is realized in Fig. 2. When the distance between the blocked level f and the next one $f + 1$ is small the blocking effect can only reduce the strength of the pairing as seen in Fig. 3.

In Fig. 4 we compare the temperature dependence of the BCS and the number-parity projected mean values of the pairing parameter $\Delta_\eta = \langle \Delta_\eta(\mathbf{r}) \rangle$ for grains with $D = 2.0094$ nm and $D = 2.0095$ nm containing $N_e = 1188$ (even case) and $N_e = 1189$ (odd case) carriers, respectively. As seen from this figure the even-N_e projected mean value of the order parameter is always larger than the BCS one. The two curves meet at $T = 0$, as expected from Eq. (17). The odd-N_e curve can for some parameters go below the BCS curve which is the case in Fig. 4. For the case of extremely small grains as in the figure, the critical temperature is raised by the even-N_e projection and lowered by the odd-N_e projection. Notice the unusual behavior of the pairing gap with temperature in the case of a nanograin with an odd number of electrons. The odd-N_e order parameter first slightly increases, then reaches a maximum, and finally decreases to zero at the critical temperature $T_c^{\eta=-1}$. In the case of the odd-N_e grain with $D = 2.0022$ nm, not shown here, the behavior of the mean value order parameter is even more dramatic: the pairing disappears below a new critical

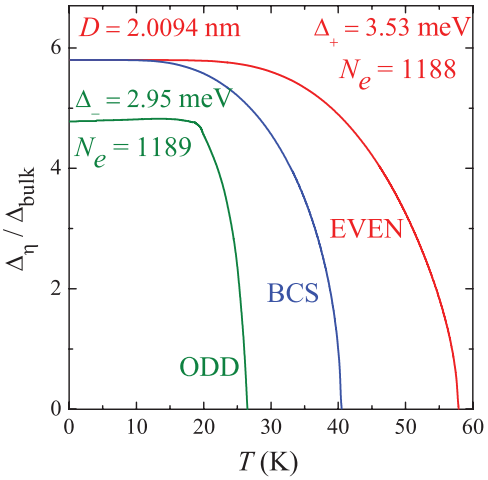

FIG. 4. (Color online) Mean value of the order parameter Δ_η as a function of temperature for the grain with size $D = 2.094$ nm.

temperature, that is, a nonvanishing order parameter exists only for intermediate temperatures. There is a re-entrance effect: superconductivity is switched off below the lower as well as above the upper critical temperature.[40]

To understand the physical reason why the temperature dependence of the order parameter significantly differs from the BCS behavior, we consider the low-temperature limit of Eq. (7). In the even case, the expansion of this equation for $\eta = +1$ yields[40]

$$\Delta_p^+ = \sum_q V_{pq} \frac{\Delta_q^+}{2\widetilde{E}_q} \left[1 - 2e^{-2\beta E_q} - 4 \sum_{r\neq p,q} e^{-\beta(E_q+E_r)} \right]. \tag{20}$$

The low temperature corrections are controlled in most cases by the second term. As in the low-temperature expansion of the BCS theory this term is negative. However, here it is proportional to $e^{-2\beta E_q}$, while in the BCS case it was $e^{-\beta E_q}$. This reflects the fact that any excitation in the even case requires the formation of an even number of quasiparticles. In the BCS theory the activation energy is directly related to the quasiparticle excitation energy via the relation $\Delta_E = \min_q(E_q)$. In exact analogy with the BCS theory, taking into account that the smallest number of quasiparticle excitations is two, we introduce the activation energy in the even case and interpret it as the minimal required excitation energy (the even excitation gap)

$$\Delta_E^+ = \min_{q,r}(2E_q, E_q + E_r). \tag{21}$$

In the BCS case, where parity is not fixed, the excitation energy is $\Delta_E^0 = \min_q(E_q)$. Since it is energetically more demanding to excite two quasiparticles than to excite one, the decrease of the order parameter with temperature in the even case is slower than that in the BCS description, which is reflected in Fig. 4.

Due to the blocking effect, for an odd number N_e of electrons, we have to consider separately the limiting cases for the levels $p \neq f$ and the pairing associated with the blocking

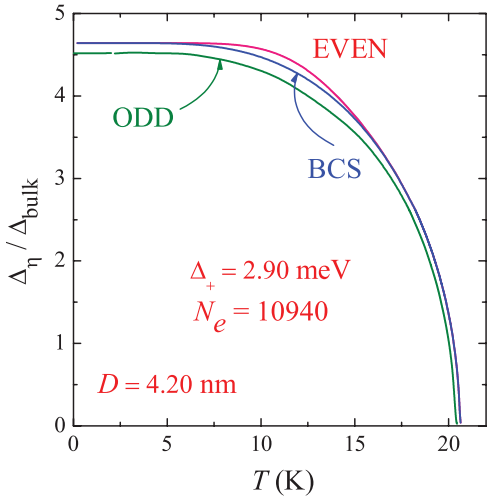

FIG. 5. (Color online) Mean value of the order parameter Δ_η as a function of temperature for a grain with size $D = 4.2$ nm.

level $p = f$.[40] Expanding Eq. (7) for $\eta = -1$ these pairing gaps are found as

$$\Delta^-_{p\neq f} = \sum_{q(q\neq f)} \left[V_{pq} \frac{\Delta^-_q}{2\widetilde{E}_q} + \left(V_{pf} \frac{\Delta^-_f}{2\widetilde{E}_f} - V_{pq} \frac{\Delta^-_q}{2\widetilde{E}_q} \right) \times e^{-\beta(E_q - E_f)} \right] \tag{22}$$

and

$$\Delta^-_{p=f} = \sum_{q(q\neq f, f+1)} \left[V_{fq} \frac{\Delta^-_q}{2\widetilde{E}_q} - g_{f+1} \left(V_{fq} \frac{\Delta^-_q}{2\widetilde{E}_q} - V_{f,f+1} \frac{\Delta^-_{f+1}}{2\widetilde{E}_{f+1}} \right) e^{-\beta(E_q - E_{f+1})} \right], \tag{23}$$

where g_{f+1} is the degeneracy of the $(f+1)$ level.

As opposed to the even case, here the low-temperature correction to the p-level pairing gap is mostly positive and governed by the exponential of the difference $E_q - E_0$. Therefore the minimal energy required to produce an excitation in the odd case is given by (the odd excitation gap)

$$\Delta^-_E = \min_q (E_q - E_f). \tag{24}$$

Thus, even if at $T = 0$ the pair formation is completely blocked for the level f, an increase of the temperature depopulates this blocked level due to the thermal excitation, resulting in an increase of the pair correlations by scattering also through this level. Since it situates in the vicinity of the chemical potential, the effect can be nonnegligible. Therefore, the pairing gap for low temperatures tends to increase while at higher temperatures it decreases. This explains the behavior of the mean value of the order parameter in the odd case as well as the parity dependence of the critical temperature as a function of sample size that is observed for ultra-small samples and illustrated in Fig. 1.

When increasing the grain size the interlevel spacing reduces and the number of single-electron levels in the Debye window around the chemical potential, within which electrons are affected by the pairing correlations, increases. Hence the importance of the blocked level diminishes. This results in the observed reduction of the parity induced differences. As was shown in Ref. 41, on average the difference between the even and odd values of the order parameter at $T = 0$ is $d/2$, where d is the mean value spacing. This is illustrated in Fig. 5, where the mean value of the order parameter is plotted vs temperature.

Above we have seen that parity influences the superconducting gap for ultra-small grains. In the even case it is equal to the BCS superconducting gap, while in the odd case it is smaller due to the blocking effect. However, note that it is the excitation gap $\Delta^\pm_E$ [see Eqs. (21) and (24)] that is measured as a spectral gap in a superconducting state via tunneling conductance in the STM experiments. Therefore it is of interest to investigate the influence of the electron number parity on the excitation gaps and their dependence on the grain thickness. Figure 6 displays the excitation gaps as a function of the grain

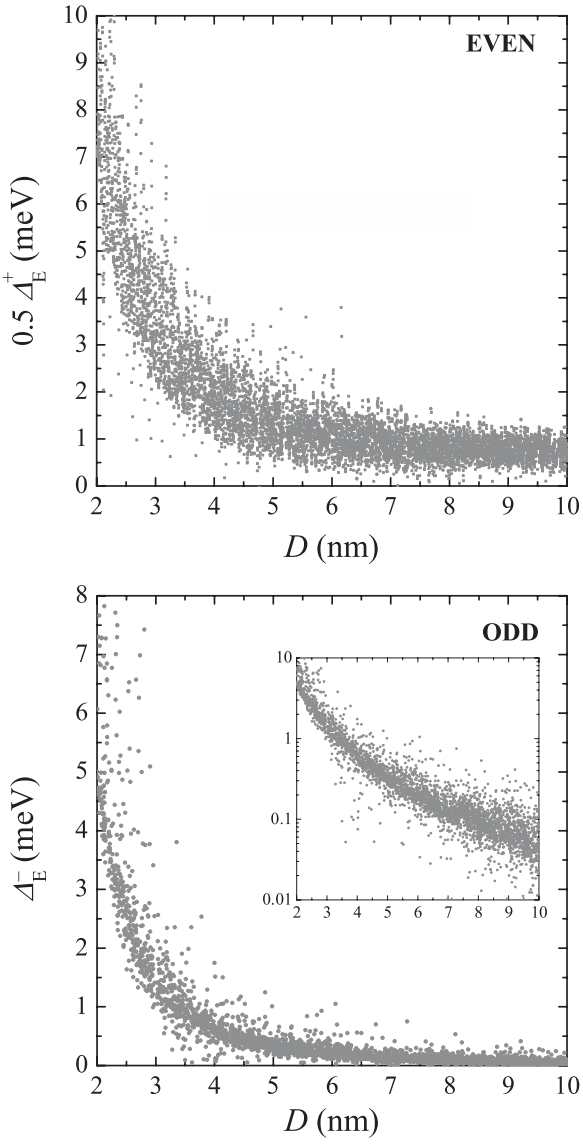

FIG. 6. Excitation gaps $\Delta^\pm_E$ as a function of the grain size D: (upper panel) for a grain with even-N_e number of carriers; (lower panel) for a grain with odd-N_e number of carriers. Inset: Δ^-_E in the logarithmic scale.

width for positive and negative parity, respectively. Here two characteristic features are worth mentioning. First, as any other quantity pertaining to nanoscale superconducting samples the excitation gaps exhibit size-dependent oscillations. Second, while Δ_E^+ approaches its bulk value 2×0.616 meV with increasing grain size, Δ_E^- vanishes for large grains, reflecting the fact that odd excitations are gapless in infinitely large systems.[37] In the even case the contribution to the excitation gap comes from both the superconducting gap (gap for the pair excitation $2\Delta_p^+$) of a certain level and also from the single-electron gap due to quantum confinement δ_p. Therefore, we can write $\Delta_E^+ = 2\min_p(\Delta_p^+ + \delta_p)$. The increase of the excitation gap with decreasing grain size is due to both these quantities. In the odd case the situation is different. As has been shown above for an odd number of carriers in the grain, the excitation gap is determined approximately by $\min_p(\sqrt{\xi_p^2 + |\Delta_p^\eta|^2} - \sqrt{\xi_0^2 + |\Delta_0^\eta|^2})$ and if we suppose that Δ_p^η does not depend on the index p (i.e., we neglect the spatial variation of the order parameter[23]) then the odd excitation gap is determined by $\min_p(|\xi_p| - |\xi_0|)$, which is simply the gap induced by confinement in the single-electron spectrum of a grain, or the smallest single particle excitation of an unpaired electron. The importance of the odd excitation gap is related to the blocking effect in the odd case and it diminished with grain size.

Having at our disposal the parity dependent excitation gaps and the superconducting critical temperature we can obtain the parity dependent coupling ratio ζ as a function of the grain size. Before discussing the impact of the two different parities, it is instructive to have a look at the size dependence of ζ in the BCS case, which can be obtained from Eqs. (8) and (9), when the parity parameter is set to $\eta = 0$. Figure 7 shows corresponding results. As seen from the figure the coupling ratio increases with decreasing grain size from its value of $\zeta = 1.76$ for large thicknesses. In most cases it approaches values near $\zeta = 2$. Exactly $\zeta = 2$ is obtained only when: (i) there is only one level in the Debye window; and (ii) this level is degenerate and coincides with the chemical potential. Apart from this main trend, for a considerable share of grain sizes the coupling ratio is well above this value. The solid curves show approximate upper and lower boundaries for the ζ oscillations.

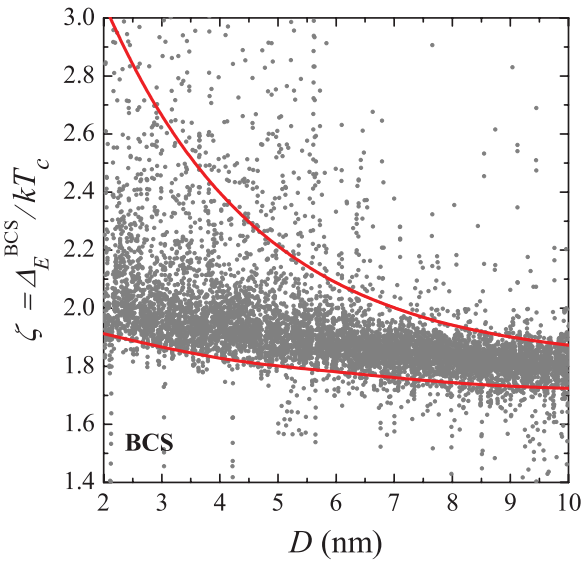

FIG. 7. (Color online) The coupling ratio $\zeta = \Delta_E/k_BT_c$ vs the grain thickness in the BCS case.

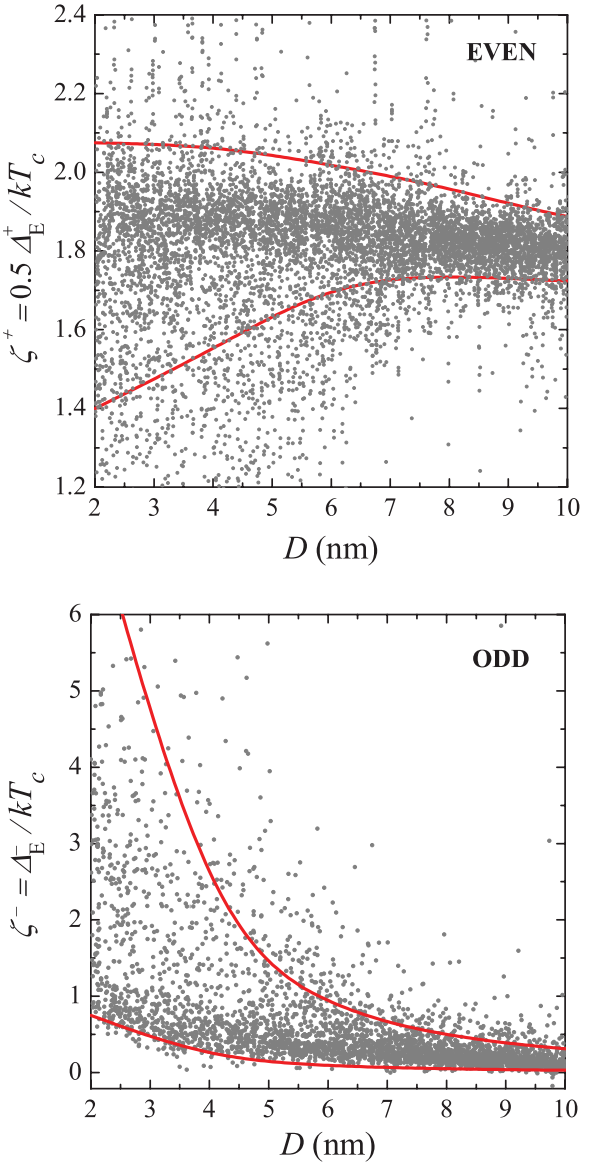

FIG. 8. (Color online) The coupling ratio $\zeta = \Delta_E/k_BT_c$ vs the grain thickness: (upper panel) even-N_e grain; (lower panel) odd-N_e grain.

Let us turn now to the parity dependence of ζ. Plotted in Fig. 8 is the coupling ratio ζ for even (upper panel) and odd (lower panel) grains, as a function of the grain width. The solid curves show approximate upper and lower boundaries for ζ. In both cases the ζ values for different grain sizes cluster densely around a position that increases for smaller grains. However, the lower boundary of ζ for an even number of electrons tend to decrease when the grain size is reduced. Taking into account that the spectroscopical gaps are equal for the even (normalized by 2) and the BCS case, this reflects the fact, already investigated above, that the superconducting critical temperature for ultra-small grain sizes can be larger

than that in the BCS case. Thus, as opposed to the BCS case for even number of electrons, ζ is below its bulk value $\zeta = 1.76$ for a significant fraction of grain sizes.

In the odd case (lower panel) ζ is zero for the bulk as expected from the above discussion and increases with decreasing grain size. This increase is purely due to the quantum confinement modification of the single-electron spectrum.

Now we discuss the possible implications of the above calculations for experiments. Experimentally the spectroscopical gap is determined from conductance measurements performed with a system consisting of STM tip/superconducting grain/BN/Rh substrate. As was indicated in Refs. 31 and 32 the junction resistance is only of the order of a few ohms. Hence it is unlikely that there is a strong Coulomb blockade in the system. Thus in the experimental realization an effective ensemble of even and odd number of electrons will be measured where the parity of the grain is not fixed. This can be taken into account by averaging the coupling ratio ζ. Assuming equal probabilities for finding even and odd number of carriers in a grain we obtain for the average

$$\zeta = \tfrac{1}{2}(\zeta^+ + \zeta^-). \tag{25}$$

In Fig. 9 the solid curves illustrate approximate upper and lower boundaries for the averaged ζ oscillations, calculated using Eq. (25), while the dotted curves are the corresponding BCS results. Thus, when accounting for the parity fluctuations in the calculations, a much stronger increase of ζ with the grain size is found. This increase is due to the increase of ζ for odd electron numbers, which is controlled by the quantum confinement. Therefore, by calculating the coupling ratio separately for the grains with even and odd number of confined electrons allows us to go beyond the classical mean field description, which is questionable in the case of ultra-small grains. Within this formalism we effectively include the effects of parity number fluctuations. The interplay of these fluctuations and quantum confinement effects is responsible for the increase of ζ.

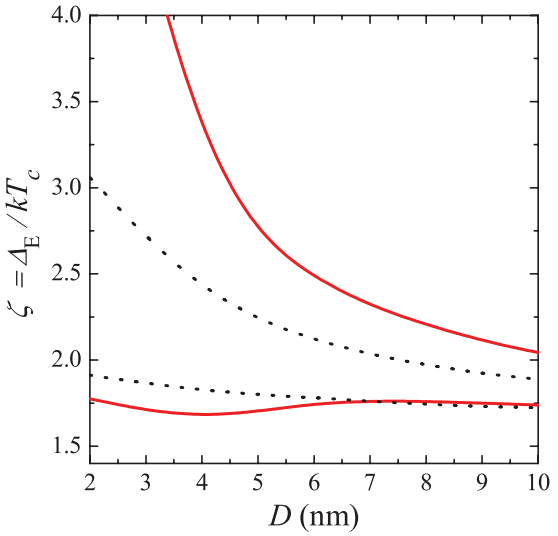

FIG. 9. (Color online) Upper and lower approximate boundaries for the oscillations of the coupling ratio $\zeta = \Delta_E / k_B T_c$ vs grain thickness. Solid line: averaged over parity. Dotted line: BCS result.

IV. CONCLUDING REMARKS

In conclusion, in this work we limited ourselves to metallic high-quality superconducting nanograins, containing more than a thousand electrons, where the quantization of the electron motion is not washed out by, for example, scattering on impurities or surface roughness. In addition, we included the spatial variation of the pair condensate and took into account the variation of the chemical potential with grain width.

Within the parity-projected BCS formalism we showed that (1) pairing in grains with an odd number of confined electrons is smaller than that in grains with an even number of electrons. In contrast, for even grains $\Delta_\eta(\mathbf{r})$ is equal to the BCS case and goes above the BCS value for finite temperatures. (2) All superconducting properties strongly oscillate with grain width, and show an overall increase with decreasing D. This results in strong oscillations of the coupling ratio in both even and odd cases. (3) The overall increase of ζ with decreasing superconducting grain size can be attributed to the interplay of parity number fluctuations of the confined electrons and a strong enlargement of the single-electron gap due to quantum confinement.

ACKNOWLEDGMENTS

This work was supported by the European Community under a Marie Curie IEF Action (Grant Agreement No. PIEF-GA-2009-235486-ScQSR), the Flamish Science Foundation (FWO-Vl), and the Belgian Science Policy (IAP). M.D.C. thanks A. S. Mel'nikov and N. B. Kopnin for fruitful discussions.

APPENDIX A: THE NUMBER-PARITY PROJECTED BCS APPROXIMATION

The equilibrium properties of the system can be derived from its grand partition function

$$Z = \mathrm{Tr}(e^{-\beta \widehat{K}}), \tag{A1}$$

where

$$\widehat{K} = \sum_p \xi_p (\widehat{a}_p^+ \widehat{a}_p + \widehat{a}_{\overline{p}}^+ \widehat{a}_{\overline{p}}) - \sum_{pq} V_{pq} \widehat{a}_p^+ \widehat{a}_{\overline{p}}^+ \widehat{a}_{\overline{q}} \widehat{a}_q. \tag{A2}$$

To shorten the formulas we assume that $V_{pp} = 0$. A nonzero value of V_{pp} entails a small state-dependent shift of the single-particle energy ξ_p, which leads to more complicated formulas but does not modify the main conclusions.

The projection which extracts the correct number parity components out of the total states is

$$\widehat{P}_\eta = \tfrac{1}{2}(\widehat{1} + \eta e^{i\pi \widehat{N}}), \tag{A3}$$

where η is equal to $+1$ for even systems and -1 for odd ones. The number-parity projected partition function is then

$$Z_\eta = \mathrm{Tr}(\widehat{P}_\eta e^{-\beta \widehat{K}}) = \tfrac{1}{2} Z(1 + \eta \langle e^{i\pi \widehat{N}} \rangle), \tag{A4}$$

Here $\xi_p = \varepsilon_p - \mu$, $\langle\widehat{\mathcal{O}}\rangle \equiv \mathrm{Tr}(\widehat{\mathcal{O}}e^{-\beta\widehat{K}})/\mathrm{Tr}(e^{-\beta\widehat{K}})$. The matrix elements of the pairing interaction, given by Eq. (2), satisfy $V_{pq} = V_{qp}$. Such an interaction scatters the pair from a fully occupied level q to another empty p level. The number-parity projected expectation value of an observable is defined as follows:

$$\langle\widehat{\mathcal{O}}\rangle_\eta \equiv \frac{\mathrm{Tr}(\widehat{\mathcal{O}}\widehat{P}_\eta e^{-\beta\widehat{K}})}{\mathrm{Tr}(\widehat{P}_\eta e^{-\beta\widehat{K}})}, \tag{A5}$$

or taking into account Eq. (A3) we find

$$\langle\widehat{\mathcal{O}}\rangle_\eta = \frac{\langle\widehat{\mathcal{O}}\rangle + \eta R_\pi \langle\widehat{\mathcal{O}}\rangle_\pi}{1+\eta R_\pi}, \tag{A6}$$

where we have used the notation

$$\langle\widehat{\mathcal{O}}\rangle_\pi \equiv \frac{\mathrm{Tr}(\widehat{\mathcal{O}}e^{i\pi\widehat{N}}e^{-\beta\widehat{K}})}{\mathrm{Tr}(e^{i\pi\widehat{N}}e^{-\beta\widehat{K}})}. \tag{A7}$$

We variationally minimize an approximate free energy $\widehat{F}$ defined by

$$\widehat{F} = \langle\widehat{H} - \widehat{H}_0\rangle_0 + \widehat{F}_0.$$

By performing the Bogoliubov transformation

$$\widehat{\gamma}_{\overline{p}} = u_p\widehat{a}_p - v_p\widehat{a}^+_{\overline{p}}, \tag{A8}$$

$$\widehat{\gamma}_p = u_p\widehat{a}_{\overline{p}} + v_p\widehat{a}^+_p, \tag{A9}$$

$$|u_p|^2 + |v_p|^2 = 1, \tag{A10}$$

one can write[41]

$$\widehat{K} = \widehat{K}_0 + \widehat{K}_Q + \widehat{K}_{\mathrm{int}}. \tag{A11}$$

Here

$$\widehat{K}_0 = 2\sum_p \xi_p v_p^2 - \frac{1}{4}\sum_{q,p} V_{qp}S_pS_q \tag{A12}$$

is the temperature dependent c-number term, where $C_p \equiv u_p^2 - v_p^2$ and $S_p \equiv 2u_pv_p$. We introduce the diagonal term (one-body operator)

$$\widehat{K}_Q = \sum_p E_p\widehat{b}_p \tag{A13}$$

with $\widehat{b}_p = \widehat{\gamma}^+_p\widehat{\gamma}_p + \widehat{\gamma}^+_{\overline{p}}\widehat{\gamma}_{\overline{p}}$, which describes the energy of the independent Bogoliubov quasiparticles with variational parameters E_p. The left interaction between the Bogoliubov quasiparticles is gathered in the term $\widehat{K}_{\mathrm{int}}$ which has the following form:

$$\widehat{K}_{\mathrm{int}} = \sum_p\left(\xi_pC_p + \frac{S_p}{2}\sum_q V_{qp}S_q - E_p\right)\widehat{b}_p - \frac{1}{4}\sum_{q,p} V_{qp}S_pS_q\widehat{b}_p\widehat{b}_q, \tag{A14}$$

Here the quantities E_p and $u_p(v_p)$ must be determined from the stationarity condition of the grand potential.

Then we make the mean field approximation by assuming that the low-temperature equilibrium properties of the system are governed by the independent quasiparticles and we work with averages

$$\langle\widehat{\gamma}^+_p\widehat{\gamma}_p\rangle = f(E_p) = [\exp(\beta E_p)+1]^{-1}. \tag{A15}$$

Hence the interaction term is replaced by its average value

$$\widehat{K} = \widehat{K}_Q + H_\eta, \tag{A16}$$

where

$$H_\eta = \langle\widehat{K}_{\mathrm{int}}\rangle_\eta + H_0. \tag{A17}$$

Let us first calculate the partition function in the absence of the interaction term

$$Z_0 = \mathrm{Tr}\exp\left(-\beta\sum_p\widehat{H}_p\right) = \mathrm{Tr}\prod_p\exp(-\beta\widehat{H}_p), \tag{A18}$$

where $\widehat{H}_p = E_p\widehat{b}_p$. However,

$$\mathrm{Tr}\prod_p\exp(-\beta\widehat{H}_p) = \prod_{p\neq\overline{p}}\mathrm{Tr}_p\exp(-\beta\widehat{H}_p), \tag{A19}$$

where Tr_p is the trace evaluated in the Fock space of the orbital pair $(p,\overline{p})$, that is, in the four-dimensional space spanned by $\{|n_p,n_{\overline{p}}\rangle\} = \{|0,0\rangle,|0,1\rangle,|1,0\rangle,|1,1\rangle\}$. In this representation we get

$$\mathrm{Tr}_p\exp(-\beta\widehat{H}_p) = 1 + 2e^{-\beta E_p} + e^{-2\beta E_p} = (1+e^{-\beta E_p})^2. \tag{A20}$$

Therefore, in this case,

$$Z_0 = \prod_{p,\sigma}(1+e^{-\beta E_p}). \tag{A21}$$

The projected partition function introduces the operator $\exp(i\pi\widehat{N})$.[52] Within each subspace $(p,\overline{p})$ changes the sign of the odd particle number vectors. Therefore

$$\mathrm{Tr}_p\widehat{P}_\eta\exp(-\beta\widehat{H}_p) = 1 - 2e^{-\beta E_p} + e^{-2\beta E_p} = (1-e^{-\beta E_p})^2. \tag{A22}$$

Therefore, in the odd case the partition function reads as

$$Z_\pi = \prod_{p,\sigma}(1-e^{-\beta E_p}). \tag{A23}$$

From the partition functions we obtain the occupation probabilities. Indeed, let us define $\Omega_{0,p}$ as the grand potential of the level p

$$\Omega_{0,p} = -\frac{1}{\beta}\ln(1-e^{-\beta E_p}). \tag{A24}$$

Since the average number of particles in the system is $\overline{n}_p = -.\frac{\partial\Omega_{0,p}}{\partial\mu}|_{\mu=0}$ we obtain the level occupation probability in the odd case

$$f_\pi(E_p) = -[\exp(\beta E_p) - 1]^{-1}. \tag{A25}$$

Hence the projected grand-canonical partition function without interaction is

$$Z_{0,\eta} = \tfrac{1}{2}Z_0\,(1+\eta R_\pi) \tag{A26}$$

with

$$R_\pi \equiv \prod_{p,\sigma} t_p = \langle e^{i\pi \widehat{N}} \rangle \tag{A27}$$

and with Eq. (A4),

$$Z_\eta = \tfrac{1}{2} Z\,(1 + \eta R_\pi)\,, \tag{A28}$$

where $Z = Z_0 \exp(H_\eta)$. Here we have introduced for shorthand the following notation:

$$t_p \equiv \tanh\left(\frac{\beta E_p}{2}\right). \tag{A29}$$

The number-parity projected grand potential can be directly obtained from the number-parity projected partition function via

$$\Omega_\eta = -\frac{1}{\beta} \ln Z_\eta = \Omega_Q + H_\eta, \tag{A30}$$

where we have introduced the short notation

$$\Omega_Q = -\frac{1}{\beta} \ln Z_0 - \frac{1}{\beta} \ln\left[\frac{1}{2}\,(1 + \eta R_\pi)\right]. \tag{A31}$$

Let us calculate each term separately. We start with

$$H_\eta = 2\sum_p \xi_p v_p^2 + \sum_p [\xi_p C_p - E_p] f_\eta(E_p) - \frac{1}{4}\sum_{q,p} V_{qp} S_p S_q [1 - 2 f_\eta(E_p)][1 - 2 f_\eta(E_q)], \tag{A32}$$

where

$$f_\eta(E_p) = \langle \widehat{\gamma}_p^+ \widehat{\gamma}_p \rangle_\eta = \frac{f(E_p) + \eta R_\pi f_\pi(E_p)}{1 + \eta R_\pi}. \tag{A33}$$

If we introduce the following notations:

$$t_p = 1 - 2 f(E_p) = \tanh\left(\frac{\beta E_p}{2}\right), \tag{A34}$$

$$t_p^{-1} = 1 - 2 f_\pi(E_p) = \coth\left(\frac{\beta E_p}{2}\right), \tag{A35}$$

then we obtain

$$H_\eta = \sum_p \xi_p \left(1 - C_p \frac{t_p + \eta R_\pi t_p^{-1}}{1 + \eta R_\pi}\right) - \sum_p E_p \frac{(1 - t_p) + \eta R_\pi \left(1 - t_p^{-1}\right)}{1 + \eta R_\pi} - \frac{1}{4}\sum_{q,p} V_{qp} S_p S_q \frac{t_p t_q + \eta R_\pi t_p^{-1} t_q^{-1}}{1 + \eta R_\pi}. \tag{A36}$$

After some rearrangements we get

$$\Omega_\eta = \Omega_Q + \frac{\Gamma + \eta R_\pi \Gamma_\pi}{1 + \eta R_\pi}, \tag{A37}$$

where

$$\Gamma \equiv \sum_p E_p (t_p - 1) + \xi_p (1 - C_p t_p) - \frac{1}{2} S_p t_p \Delta_p^0 \tag{A38}$$

and

$$\Gamma_\pi \equiv \sum_p E_p \left(t_p^{-1} - 1\right) + \xi_p \left(1 - C_p t_p^{-1}\right) - \frac{1}{2} S_p t_p^{-1} \Delta_p^\pi. \tag{A39}$$

Here we have introduced

$$\Delta_p^0 \equiv \frac{1}{2}\sum_q V_{pq} S_q t_q \tag{A40}$$

and

$$\Delta_p^\pi \equiv \frac{1}{2}\sum_q V_{pq} S_q t_q^{-1}. \tag{A41}$$

The grand potential is a functional of two independent functions, say E_p and v_p, and thus $\Omega_\eta = \Omega_\eta(\{E_p, v_p\})$. Minimization with respect to these parameters gives two variational equations, which in the BCS case yield the energy spectrum and the gap equation. We follow the same strategy. First let us take the derivative of Ω_η with respect to v_p

$$\frac{\partial}{\partial v_p}\Omega_\eta = \frac{1}{1 + \eta R_\pi}\left(\frac{\partial}{\partial v_p}\Gamma + \eta R_\pi \frac{\partial}{\partial v_p}\Gamma_\pi\right) = 0 \tag{A42}$$

and we obtain the first equation

$$\xi_p S_p - C_p \Delta_p^\eta = 0, \tag{A43}$$

where[40]

$$\Delta_p^\eta = \frac{\Delta_p^0 + \eta R_\pi \Delta_p^\pi t_p^{-2}}{1 + \eta R_\pi t_p^{-2}}. \tag{A44}$$

Next we take the derivative of Ω_η with respect to E_p. With the help of the following derivatives:

$$\frac{\partial}{\partial E_p} R_\pi = \beta\left(t_p^{-1} - t_p\right) R_\pi, \tag{A45}$$

$$\frac{\partial}{\partial E_p} t_p = \frac{\beta}{2}\left(1 - t_p^2\right), \tag{A46}$$

$$\frac{\partial}{\partial E_p} t_p^{-1} = \frac{\beta}{2}\left(1 - t_p^{-2}\right), \tag{A47}$$

$$\frac{\partial}{\partial E_p}\frac{1}{1 + \eta R_\pi} = -\beta \eta R_\pi \frac{\left(t_p^{-1} - t_p\right)}{(1 + \eta R_\pi)^2}, \tag{A48}$$

$$\frac{\partial}{\partial E_p}\Omega_Q = \frac{(1 - t_p) + \eta R_\pi \left(1 - t_p^{-1}\right)}{1 + \eta R_\pi}, \tag{A49}$$

together with

$$\frac{\partial}{\partial E_p}\Gamma = (t_p - 1) + \frac{\beta}{2}\left(1 - t_p^2\right)\left(E_p - \xi_p C_p - S_p \Delta_p^0\right) \tag{A50}$$

and

$$\frac{\partial}{\partial E_p}\Gamma_\pi = \left(t_p^{-1} - 1\right) + \frac{\beta}{2}\left(1 - t_p^{-2}\right)\left(E_p - \xi_p C_p - S_p \Delta_p^\pi\right) \tag{A51}$$

we obtain

$$\frac{\partial}{\partial E_p}\Omega_\eta = \beta\eta R_\pi \frac{\left(t_p^{-1}-t_p\right)}{(1+\eta R_\pi)^2}(\Gamma_\pi-\Gamma)+\frac{\beta/2}{1+\eta R_\pi} \times\left\{(E_p-\xi_p C_p)\left[(1-t_p)+\eta R_\pi\left(1-t_p^{-1}\right)\right] - S_p\left[\Delta_p^0(1-t_p)+\eta R_\pi\left(1-t_p^{-1}\right)\Delta_p^\pi\right]\right\}. \quad \text{(A52)}$$

With some rearrangements this leads to

$$\Gamma_\pi-\Gamma=\sum_q\left(t_q^{-1}-t_q\right)\left[E_q-\xi_q C_q-\frac{1}{2}S_q\left(\Delta_q^0+\Delta_q^\pi\right)\right] \quad \text{(A53)}$$

and finally we obtain the second equation

$$E_p=\xi_p C_p+S_p\Delta_p^{-\eta}-\frac{2\eta R_\pi \mathcal{K}}{t_p-\eta R_\pi t_p^{-1}}, \quad \text{(A54)}$$

where

$$\Delta_p^{-\eta}=\Delta_p^\eta-\frac{2\eta R_\pi\left(\Delta_p^\pi-\Delta_p^0\right)}{t_p^2-R_\pi^2 t_p^{-2}} \quad \text{(A55)}$$

and

$$\mathcal{K}=\frac{\Gamma_\pi-\Gamma}{1+\eta R_\pi}. \quad \text{(A56)}$$

Making use of the relation

$$C_p^2+S_p^2=1, \quad \text{(A57)}$$

Eq. (A43) can be rewritten as

$$\frac{S_p}{\Delta_p^\eta}=\frac{C_p}{\xi_p}=\frac{1}{\widetilde{E}_p} \quad \text{(A58)}$$

with $\widetilde{E}_p$ having the familiar BCS form

$$\widetilde{E}_p\equiv\sqrt{\xi_p^2+\left|\Delta_p^\eta\right|^2} \quad \text{(A59)}$$

and hence

$$E_p=\widetilde{E}_p-\frac{2\eta R_\pi\mathcal{K}}{t_p-\eta R_\pi t_p^{-1}}-\frac{2\eta R_\pi\left(\Delta_p^\pi-\Delta_p^0\right)}{t_p^2-R_\pi^2 t_p^{-2}}\frac{\Delta_p^\eta}{\widetilde{E}_p}. \quad \text{(A60)}$$

We can eliminate C_p and S_p from the definition of Δ_p^η (A44) and $\Delta_p^\pi-\Delta_p^0$. Finally we get[40]

$$\Delta_p^\pi-\Delta_p^0\equiv\sum_q V_{pq}\frac{\Delta_q^\eta\left(t_q^{-1}-t_q\right)}{2\widetilde{E}_q} \quad \text{(A61)}$$

and

$$\Delta_p^\eta=\sum_q V_{pq}\frac{\Delta_q^\eta t_q}{2\widetilde{E}_q}\frac{1+\eta R_\pi t_p^{-2}t_q^{-2}}{1+\eta R_\pi t_p^{-2}}. \quad \text{(A62)}$$

Hence we obtained the following equations that have to be solved self-consistently:

$$E_p=\widetilde{E}_p-\frac{2\eta R_\pi}{t_p-\eta R_\pi t_p^{-1}}\left[\mathcal{K}+\frac{\left(\Delta_p^\pi-\Delta_p^0\right)}{t_p+\eta R_\pi t_p^{-1}}\frac{\Delta_p^\eta}{\widetilde{E}_p}\right], \quad \text{(A63)}$$

$$\Delta_p^\pi-\Delta_p^0\equiv\sum_q V_{pq}\frac{\Delta_q^\eta\left(t_q^{-1}-t_q\right)}{2\widetilde{E}_q}, \quad \text{(A64)}$$

$$\Delta_p^\eta=\sum_q V_{pq}\frac{\Delta_q^\eta t_q}{2\widetilde{E}_q}\left[1-\frac{\eta R_\pi t_p^{-2}\left(1-t_q^{-2}\right)}{1+\eta R_\pi t_p^{-2}}\right], \quad \text{(A65)}$$

and

$$\mathcal{K}=\frac{1}{2}\frac{\sum_q t_q D_q\left(1+\eta R_\pi t_q^{-2}\right)\left(\Delta_q^\pi-\Delta_q^0\right)\frac{\Delta_q^\eta}{\widetilde{E}_q}}{1+\eta R_\pi\left(1-2\sum_q D_q\right)} \quad \text{(A66)}$$

with

$$D_q=1-t_q^{-2}\frac{1-\eta R_\pi}{1-\eta R_\pi t_q^{-2}}. \quad \text{(A67)}$$

APPENDIX B: THE SPATIAL VARIATION OF THE ORDER PARAMETER

From the numerical procedure we obtain the order parameter. According to the definition of the order parameter

$$\Delta(\mathbf{r})=g\langle\psi_\uparrow\psi_\downarrow\rangle. \quad \text{(B1)}$$

Performing the Bogoliubov transformation

$$\psi_\uparrow(\mathbf{r})=\sum_p[u_p(\mathbf{r})\widehat{\gamma}_p+v_p^*(\mathbf{r})\widehat{\gamma}_{\overline{p}}^+],$$
$$\psi_\downarrow(\mathbf{r})=\sum_p[u_p(\mathbf{r})\widehat{\gamma}_{\overline{p}}-v_p^*(\mathbf{r})\widehat{\gamma}_p^+] \quad \text{(B2)}$$

and making use of the fact that the averaging procedure $\langle\widehat{\mathcal{O}}\rangle\equiv\mathrm{Tr}(\widehat{\mathcal{O}}e^{-\beta\widehat{K}_Q})/\mathrm{Tr}(e^{-\beta\widehat{K}_Q})$ is performed with respect to the Hamiltonian $\widehat{K}_Q$, which commutes with the N operator and we get

$$\Delta(\mathbf{r})=g\sum_p u_p(\mathbf{r})v_p^*(\mathbf{r})[1-2f_\eta(E_p)] \quad \text{(B3)}$$

or

$$\Delta(\mathbf{r})=g\sum_p u_p(\mathbf{r})v_p^*(\mathbf{r})\frac{t_p+\eta R_\pi t_p^{-1}}{1+\eta R_\pi}. \quad \text{(B4)}$$

In the Anderson approximation $u_p(\mathbf{r})=U_p\varphi_p(\mathbf{r})$ and $v_p(\mathbf{r})=V_p\varphi_p(\mathbf{r})$ and therefore

$$\Delta(\mathbf{r})=g\sum_p|\varphi_p(\mathbf{r})|^2\frac{\Delta_p^\eta}{2\widetilde{E}_p}t_p\left(1-\eta R_\pi\frac{1-t_p^{-2}}{1+\eta R_\pi}\right). \quad \text{(B5)}$$

[1] R. Parmenter, Phys. Rev. **166**, 392 (1968).
[2] J. M. Blatt and C. J. Thompson, Phys. Rev. Lett. **10**, 332 (1963).
[3] B. Mühlschlegel, D. J. Scalapino, and R. Denton, Phys. Rev. B **6**, 1767 (1972).
[4] R. A. Smith and V. Ambegaokar, Phys. Rev. Lett. **77**, 4962 (1996).
[5] A. Perali, A. Bianconi, A. Lanzara, and N. L. Saini, Solid State Commun. **100**, 181 (1996).
[6] F. Braun and J. von Delft, Phys. Rev. B **59**, 9527 (1999).
[7] G. Sierra, J. Dukelsky, G. G. Dussel, J. von Delft, and F. Braun, Phys. Rev. B **61**, R11890 (2000).

[8]V. N. Gladilin, V. M. Fomin, and J. T. Devreese, Solid State Commun. **121**, 519 (2002); Phys. Rev. B **70**, 144506 (2004).
[9]E. A. Yuzbashyan, A. A. Baytin, and B. L. Altshuler, Phys. Rev. B **68**, 214509 (2003).
[10]Y. N. Ovchinnikov and V. Z. Kresin, Eur. Phys. J. B **45**, 5 (2005); Eur. Phys. J. B **47**, 333 (2005).
[11]V. Z. Kresin and Y. N. Ovchinnikov, Phys. Rev. B **74**, 024514 (2006).
[12]A. A. Shanenko and M. D. Croitoru, Phys. Rev. B **73**, 012510 (2006).
[13]M. D. Croitoru, A. A. Shanenko, and F. M. Peeters, Phys. Rev. B **76**, 024511 (2007).
[14]D. Innocenti, N. Poccia, A. Ricci, A. Valletta, S. Caprara, A. Perali, and A. Bianconi, Phys. Rev. B **82**, 184528 (2010).
[15]Y. Guo, Y.-F. Zhang, X.-Y. Bao, T.-Z. Han, Z. Tang, L.-X. Zhang, W.-G. Zhu, E. G. Wang, Q. Niu, Z. Q. Qiu, J.-F. Jia, Z.-X. Zhao, and Q.-K. Xue, Science **306**, 1915 (2004).
[16]Y.-F. Zhang, J.-F. Jia, T.-Z. Han, Z. Tang, Q.-T. Shen, Y. Guo, Z. Q. Qiu, and Q.-K. Xue, Phys. Rev. Lett. **95**, 096802 (2005).
[17]X.-Y. Bao, Y.-F. Zhang, Y. Wang, J.-F. Jia, Q.-K. Xue, X. C. Xie, and Z.-X. Zhao, Phys. Rev. Lett. **95**, 247005 (2005).
[18]D. C. Ralph, C. T. Black, and M. Tinkham, Phys. Rev. Lett. **74**, 3241 (1995).
[19]C. T. Black, D. C. Ralph, and M. Tinkham, Phys. Rev. Lett. **76**, 688 (1996).
[20]A. A. Shanenko, M. D. Croitoru, R. G. Mints, and F. M. Peeters, Phys. Rev. Lett. **99**, 067007 (2007).
[21]M. D. Croitoru, A. A. Shanenko, and F. M. Peeters, Int. J. Mod. Phys. B **23**, 4257 (2009).
[22]M. D. Croitoru, A. A. Shanenko, C. C. Kaun, and F. M. Peeters, Phys. Rev. B **80**, 024513 (2009).
[23]M. D. Croitoru, A. A. Shanenko, C. C. Kaun, and F. M. Peeters, Phys. Rev. B **83**, 214509 (2011).
[24]I. Giaever and H. R. Zeller, Phys. Rev. Lett. **20**, 1504 (1968); H. R. Zeller and I. Giaever, Phys. Rev. **181**, 789 (1969).
[25]W.-H. Li, C. C. Yang, F. C. Tsao, S. Y. Wu, P. J. Huang, M. K. Chung, and Y. D. Yao, Phys. Rev. B **72**, 214516 (2005).
[26]W.-H. Li, C.-W. Wang, C.-Y. Li, C. K. Hsu, C. C. Yang, and C.-M. Wu, Phys. Rev. B **77**, 094508 (2008).
[27]B. Abeles, Adv. Phys. **24**, 407 (1975).
[28]Y. Shapira and G. Deutscher, Thin Solid Films **87**, 29 (1982).
[29]Y. Shapira and G. Deutscher, Phys. Rev. B **27**, 4463 (1983).
[30]S. Bose, P. Raychaudhuri, R. Banerjee, P. Vasa, and P. Ayyub, Phys. Rev. Lett. **95**, 147003 (2005).
[31]S. Bose, C. Galande, S. Chockalingam, R. Banerjee, P. Raychaudhuri, and P. Ayyub, J. Phys. Condens. Matter **21**, 205702 (2009).
[32]I. Brihuega, S. Bose, M. M. Ugeda, C. H. Michaelis, and K. Kern, Phys. Rev. B **84**, 104525 (2011); S. Bose, A. M. García-García, M. M. Ugeda, J. D. Urbina, C. H. Michaelis, I. Brihuega, and K. Kern, Nat. Mater. **9**, 550 (2010).
[33]M. V. Feigel'man, L. B. Ioffe, V. E. Kravtsov, and E. A. Yuzbashyan, Phys. Rev. Lett. **98**, 027001 (2007).
[34]S. Bose, and P. Raychaudhuri (private communication).
[35]R. W. Richardson, Phys. Lett. **3**, 277 (1963).
[36]K. Dietrich, H. J. Mang, and J. H. Pradal, Phys. Rev. **135**, B22 (1964).
[37]A. Mastellone, G. Falci, and R. Fazio, Phys. Rev. Lett. **80**, 4542 (1998).
[38]F. Braun and J. von Delft, Phys. Rev. Lett. **81**, 4712 (1998).
[39]J. Dukelsky and G. Sierra, Phys. Rev. Lett. **83**, 172 (1999).
[40]R. Balian, H. Flocard, and M. Veneroni, Phys. Rep. **317**, 251 (1999).
[41]B. Janko, A. Smith, and V. Ambegaokar, Phys. Rev. B. **50**, 1152 (1994).
[42]D. S. Golubev and A. D. Zaikin, Phys. Lett. A **195**, 380 (1994).
[43]S. D. Berger and B. I. Halperin, Phys. Rev. B **58**, 5213 (1998).
[44]K. A. Matveev and A. I. Larkin, Phys. Rev. Lett. **78**, 3749 (1997).
[45]M. T. Tuominen, J. M. Hergenrother, T. S. Tighe, and M. Tinkham, Phys. Rev. Lett. **69**, 1997 (1992).
[46]P. Lafarge, P. Joyez, D. Esteve, C. Urbina, and M. H. Devoret, Phys. Rev. Lett. **70**, 994 (1993).
[47]N. N. Bogoliubov, Sov. Phys.-Usp. **2**, 236 (1959) [see also, N. N. Bogoliubov, *Selected Works, Part II, Quantum and Classical Statistical Mechanics* (Gordon and Breach, Amsterdam, 1991)].
[48]P. G. de Gennes, *Superconductivity of Metals and Alloys* (W. A. Benjamin, New York, 1966).
[49]A. L. Fetter and J. D. Walecka, *Quantum Theory of Many-Particle Systems* (Dover, New York, 2003).
[50]J. von Delft, A. D. Zaikin, D. S. Golubev, and W. Tichy, Phys. Rev. Lett. **77**, 3189 (1996).
[51]V. G. Soloviev, Kgl. Dan. Vid. Selsk., Mat.-Fys. Skr. **1**(11), 1 (1961); P. Ring and P. Schuck, *The Nuclear Many-Body Problem* (Springer-Verlag, New York, 1980).
[52]Y. Alhassid, G. F. Bertsch, L. Fang, and S. Liu, Phys. Rev. C **72**, 064326 (2005).